Volumetric Assessment of Fatigue Damage in a SiC_f/SiC Ceramic Matrix Composite via In Situ X-ray Computed Tomography

Zak Quiney [1*], Eleri Weston [2], P. Ian Nicholson [2], Stephen Pattison [3], Martin R. Bache [1]

[1] Institute of Structural Materials, College of Engineering, Swansea University, Swansea SA1 8EN, UK

[2] TWI Technology Centre Wales, Harbourside Business Park, Harbourside Road, Port Talbot SA13 1SB, UK

[3] Rolls-Royce plc, P.O. Box 31, Derby DE24 8BJ, UK

*Corresponding author at: Institute of Structural Materials, College of Engineering, Swansea University, Swansea SA1 8EN, UK. *Email address:* z.a.quiney@swansea.ac.uk (Z. Quiney)

Abstract

To enhance the understanding of matrix cracking and damage progression on the macroscopic scale, within a 0/90º fibre reinforced SiC_f/SiC ceramic matrix composite (CMC), X-ray computed tomography (XCT) imaging and analysis have been performed in conjunction with a commercially available in-situ mechanical loading device. CMC test coupons were subjected to tensile cyclic loads and inspected using XCT without removal from the tensile loading device. Attempts to measure and quantify the resulting damage using volumetric image analysis techniques are presented, by characterising the crack network from XCT images acquired at both the maximum and minimum load condition during selected fatigue cycles. The XCT detection of significant crack development within the first loading half-cycle shows good agreement with cumulative acoustic emission energy data recorded under similar test conditions. The results are seen as an important step towards correlating the damage behaviour detected via different NDE and health monitoring techniques.

1. Introduction

Ceramic matrix composites (CMCs) are attractive materials for selected high performance engineering applications due to their thermal properties, corrosion resistance, low density compared to metals, and increased toughness compared to monolithic ceramics. In order to fully assess their suitability, a detailed understanding of the complex damage initiation and accumulation mechanisms under typical mechanical loading conditions is vital. The accepted pattern of damage evolution from the initiation of matrix cracks to fibre failure and final rupture is reasonably well-documented [1] and there is now a considerable effort to utilise various non-destructive evaluation (NDE) techniques in order to visualise and assess the degree of damage that exists under a variety of loading conditions.

It is common to correlate the results of multiple NDE techniques for validation of any conclusions drawn. Initial attempts to inspect damage accumulation via X-ray computed tomography (XCT) with simultaneous acoustic emission (AE) and electrical resistance (ER) measurements have been made employing interrupted fatigue tests, where specimens are periodically removed from a test frame and transferred to an independent XCT system [2].

More recent investigations have taken place utilising a commercial in situ loading device to apply incremental monotonic tensile [3] and fatigue loading [4] to SiC_f/SiC CMC specimens, in order to acquire images of macroscopic damage progression. Other authors have used synchrotron radiation sources to acquire higher resolution in situ XCT images of CMCs [5,6], but this adversely restricts the available field of view to the microscale. In situ digital image correlation (DIC) and scanning electron microscope (SEM) imaging techniques have also been demonstrated [7], but are restricted to surface measurements. Visually, XCT provides an unrivalled depiction of damage within the internal structure of a CMC, however, it can be difficult to obtain quantifiable measurements of overall damage from the analysis. The variability of damage throughout a 3-dimensional volume complicates the traditional 2-dimensional measurements of crack density, crack length and crack opening displacement and becomes very time-consuming.

It is relatively straightforward to obtain a range of quantifiable measurements from AE analysis, but currently it is not understood to the degree that the presence and severity of individual or collective damage modes can be accurately identified from this technique alone. While there is significant research in the area of AE damage characterisation in composite materials [6,8-11], it is necessary to validate these results via visual interpretation of the corresponding XCT, SEM or destructive fractography imaging.

This paper investigates a method of visualising and quantifying 3-D damage accumulation during progressive fatigue cycles, using digital volume files obtained via in situ XCT. The variability of measurements under both relaxed and fully loaded conditions is examined. Sensitivity to surface condition is also considered through the characterisation of a CMC panel deliberately processed with distinct differences in the topography of the opposing panel surfaces. AE results obtained from additional specimens under equivalent stress conditions were also employed to confirm previous assumptions that significant matrix cracking is induced during the first half-cycle of fatigue tests.

2. Materials and methods

2.1. Experimental methods

The XCT and in situ loading system used in this research has been detailed previously [4]. The Deben CT5000 was primarily operated in load control, transferring to displacement control for the duration of each XCT scan. For fatigue testing, a triangular waveform with 100s period and load ratio of R=0.01 was employed. Absolute applied stresses cannot be quoted, suffice to say that the magnitude of P_{max} was selected to be above the proportional limit but below the UTS of the material. Based on previous results and published literature it was assumed that matrix cracking would be induced during the first fatigue cycle, although this had not been visually confirmed in our laboratory up to this point. In the current tests, XCT scans of the coupon were obtained prior to the experiments and subsequently performed at the peak (P_{max}) of cycle numbers 1, 3, 7, 15, 31, 63 and 650. A final scan was then performed at zero load (P_0) after cycle 650 in order to assess the effect of crack closure on the characterisation of prior damage. All testing was performed at room temperature.

AE data are not currently captured during our in situ XCT experiments. However, separate AE data were obtained from a standalone test in which a specimen of the same material but approximately twice the cross-sectional area was subjected to the same number of fatigue cycles at room temperature utilising a standard mechanical test rig.

The peak tensile stress in this test was approximately 90% of the peak stress experienced by the in situ XCT specimen. AE was captured via a single PAC WD sensor coupled directly to the specimen surface, amplified at 40dB and logged in a LabVIEW-based system that enabled analysis of the cumulative energy parameter.

2.2. Specimen Design and XCT Settings

The specimen geometry was dictated by the standard gripping design and load capability of the Deben in situ device. Gauge dimensions were purposefully chosen to enable a macroscopic study of damage evolution that is somewhat representative of service components. Specimens were electro-discharge machined from 16-ply 0-90° 2-D woven Hi-Nicalon^{TM} SiC$_f$/SiC CMC flat plate, approximate thickness 4.5mm. An example of a cut specimen is shown in Figure 1. The parallel section of the gauge measured 5mm in length and 5mm width, providing an aspect ratio of 1:1 and thus a similar penetration of X-ray radiation throughout the 360° rotation. During each XCT scan, the field of view extended approximately 1mm either side of the 5mm gauge length, however, for the purposes of damage quantification only the region bounded by the parallel gauge was considered. An overview of the XCT system settings including the resulting voxel resolution is provided in Table 1. The specimens were gripped to either end using a pinned keep plate mechanism, approximately midway along the load train.

Figure 1. CMC specimen geometry and key gauge dimensions.

Table 1. XCT Parameters used during scanning

X-Ray Parameter	Value
Voltage kV	80
Current (μA)	160
Filters	1mm aluminium
Exposure time (ms)	1000
Projections	2000
Source to object distance (mm)	50
Source to detector distance (mm)	1150
Voxel size (mm)	0.0091

3. Results

3.1. Conventional Imaging

Image reconstruction was performed using OEM-supplied CTPro software. The resulting digital volume files were visualised using VGStudioMax software. A typical 3-D view of the external surfaces of the scanned

specimen is shown in Figure 2, indicating the surfaces that will be referred to as the 'front' and "side" as well as the orientation of x, y and z axes.
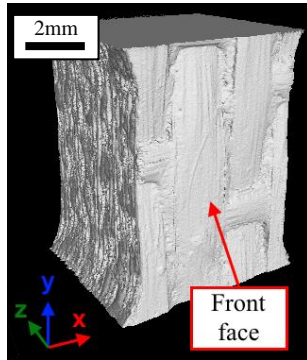

Figure 2. Three-dimensional XCT image of the "front" and "side" surfaces of the gauge section prior to loading.

Using simple 2D imaging, Figure 3 provides observations of the damage evolution taken from a single fatigue specimen, sampled at the following stages of the test: a) reference (prior to loading); b) at P_{max} cycle 1; c) at P_{max} cycle 650; and d) at P_0 cycle 650. At each stage, the images are presented from an identical subsurface plane, approximately 0.3mm beneath the front surface of the specimen.

The sequence of images in Figure 3 confirm that no pre-existing cracks existed in the specimen prior to load cycle 1. Previous incremental monotonic tensile tests on this same CMC variant have indicated that matrix cracking initiates somewhere between 25% and 50% of P_{max} [4], so the presence of matrix cracking at P_{max} of cycle 1 is not surprising. However, it does appear that a significant proportion of the transverse matrix crack network visible after 650 load cycles was already introduced during the first cycle, with the major difference in the appearance of the damage being an increase in crack opening displacements rather than the extension of existing cracks or initiation of new cracks. Comparing Figure 3c) and 3d), upon un-loading, a number of cracks were no longer visible due to crack closure, although a permanent strain causes some cracks to remain open and visible.

General observations from 2-D image analysis echo those made in prior publications [3,4], in which it was noted that the majority of cracking visible at this resolution appeared to initiate at the machined edges of the specimen and propagate inwards. Analysis of the reference image allowed a measurement of the nominal void volume within the CMC under investigation at 1.5%. Low aspect ratio voids, typically observed in matrix-rich regions or at the intersections of transverse and longitudinal tows, appeared to have minimal influence on the initiation of subsequent cracks when inspected at this spatial resolution. The same observation was previously made in similar SiC_f/SiC material containing higher levels of porosity [12]. High aspect ratio voids, typically observed within the fibre tows, sometimes appeared to interact with adjacent matrix cracks also orientated in the transverse direction. It was previously noted that 2-D crack density increased within the bounds of transverse fibre tows compared to regions of matrix material under stepped tensile loading conditions [4]. It is acknowledged that crack widths below the voxel size cannot be detected and therefore the full extent of cracking may not been visualised. In future it may be necessary to explore correlations between the measured volumetric crack content via XCT and crack density measured via SEM imaging, and this is an active area of investigation within our labs [13]. Since crack density has a good correlation with tensile stress (and also with cumulative AE energy) [14], further investigations

have been planned to assess the degree of accuracy and reliability of these volumetric crack quantifications, and also to investigate mechanical properties and remnant life predictions.
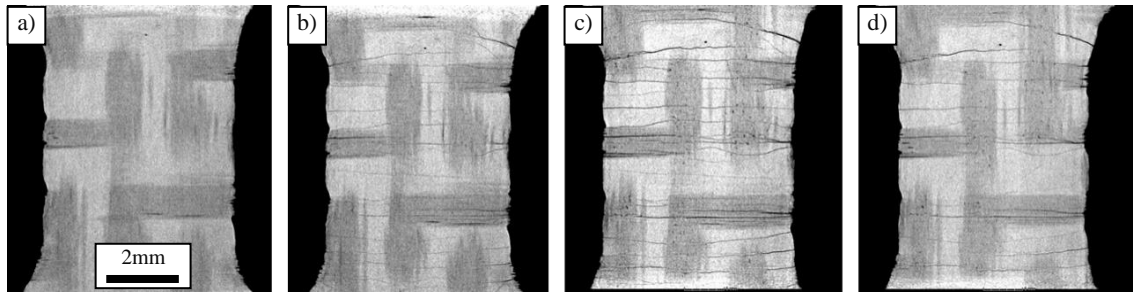

Figure 3. Subsurface damage observed on a common plate; a) prior to loading ('reference'), b) first load cycle, P_{max}, c) cycle 650, P_{max}, d) cycle 650, P_0.

3.2. *Novel Imaging and Damage Quantification*

One drawback of reporting XCT results using 2D image "slices" extracted from the volume data, such as those selected for Figure 3, is that only a single subsurface plane is represented. By viewing a dynamic sequence of different planes, the observer can detect considerable variation in the form and distribution of cracks within the network throughout the thickness of the specimen. Comparing multiple planes rapidly increases the number of images that must be correlated and at this voxel resolution more than 500 planes were available for inspection between the front and rear surfaces.

Therefore, a novel technique was developed to partition regions of damage (cracks) from the surrounding CMC structure. This was based on an image analysis threshold principles, selecting pixels below an appropriate threshold according to their numerical grayscale value. In XCT images, pixels associated with high levels of X-ray penetration (i.e. open space or very low density) are associated with a low value (dark), and pixels representing solid, dense material have a high value (light). However, attempting to characterise cracking in a CMC is problematic due to the presence of processing artefacts including porosity, incomplete infiltration between fibre bundles and between within tows, plus a general density variation which can affect local grayscale values throughout the composite volume. This newly presented technique is now demonstrated for the specimen previously characterised in Figure 3.

Returning to the original XCT data, a "stack" of 2-D images was exported from VGStudioMax, with each of the 500 images representing a different subsurface plane sampled from 'front' to 'rear' through the specimen. In order to reduce the stack to a manageable number, images were retained at a separation distance of 0.1mm, resulting in a stack of 50 images between the opposing surfaces. Referring back to Figure 2, this effectively reduced the spatial resolution in the z-direction by a factor of 10, while retaining maximum pixel resolution in the x and y-directions. This was repeated at each stage of the test selected for analysis, ensuring that each stack contained a record from identical subsurface planes.

The image stacks were then imported into SPIERS Edit software, which allows a number of threshold and image manipulation techniques to be applied to individual images or the entire stack. These can subsequently be

reconstructed into 3-D volumes within SPIERS View, where the selected pixels (voxels) can be visualised and counted.

Applying this technique, the damage introduced after 650 cycles of loading was quantified via correlations between the reference scans on each of the 50 selected 2-D planes and their equivalent scans recorded at P_{max} at N=650. Figure 4 illustrates the threshold technique applied to a single sub-surface plane imaged prior to testing. Figures 4a and 4b compare the original XCT and binary threshold images respectively, thereby identifying a distribution of inherent process artefacts for subsequent analysis. The same routine was applied after N=650 cycles, Figures 5a and 5b. For precise information, the threshold level to produce these binary images was set to 78 (on a 0 to 255 greyscale). After repeating the routine on all 50 images in the stack, the "active" pixels detected from the N=650 images were exported to a new 'object' in the SPIERS View application. The result effectively provides an inverse 3-D visualisation of the specimen gauge section after this period of fatigue cycles, Figure 6. A complex network of active pixels is noted within the bounds of the specimen, with the surrounding free space represented by the solid grey regions to either side. Notably, in this form, the resultant image was dominated by the inherent process features and provides limited capability for the observation of new cracks.

Even though the introduction of the matrix cracking may be difficult to partition from the visual presentation in Figure 6, a comparison between the number of active pixels (voxels) before and after fatigue loading can provide a quantitative measurement of the associated damage, Table 2. The total number of voxels sampled was calculated from the dimensions of each 2-D image (780x829 pixels) multiplied by the number of images in the stack (50). The difference in the volume of active pixels before and after fatigue loading at 206,737 was 0.64%. This corresponded to new damage in the form of matrix cracking.

Table 2. Voxel measurements to quantify the volume of damage (cracks) introduced by 650 fatigue cycles. Images recorded at P_{max} compared to the reference scan prior to loading).

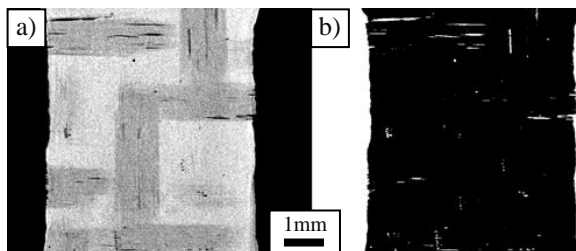|	Reference	N = 650 (P_{max})
Total voxels in volume	32,331,000	32,331,000
"Active" voxels in object	10,522,558	10,729,295
Active voxel increase at N = 650, P_{max}	206,737 (0.64% of total volume)	

Figure 4. (a) CT image, (b) equivalent threshold binary image, from an identical sub-surface plane, reference condition N=0.
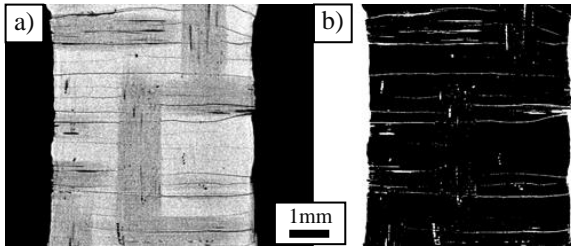
Figure 5. (a) CT image, (b) equivalent threshold binary image, from an identical sub-surface plane, recorded at P_{max} N=650.
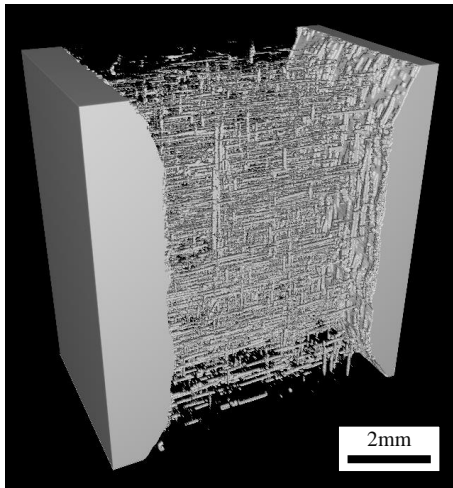

Figure 6. Three-dimensional visualisation of all active voxels within the specimen gauge at N = 650, P_{max}.

3.3. Detection of crack closure

The threshold imaging technique was also adopted as a means to quantify the intrinsic effects of crack closure. The results obtained from the stack of 50 images recorded at N=650 P_{max} were compared with similar data from a stack of 50 images obtained immediately after unloading back to zero stress.

On this occasion, no reference scan was used. Instead, the same threshold technique as above was applied, then the image was manually manipulated using the "brush" and "eraser" tools to add or remove activated pixels until only those associated with cracks remained (i.e. any features that obviously related to processing artefacts were removed). This was reasonably time consuming and reliant upon subjective interpretation, but produced a far superior result (Figure 7). For each specimen two 'objects' were exported to SPIERS View: one containing the active pixels associated with cracking (highlighted in yellow), and one containing the active pixels associated with the surrounding solid material (represented in various greyscales - obtained separately by setting a single threshold value for the entire image stack). After combining the two "objects", the transparency value of the solid body was set to 75% to enable visualisation of the internal crack network. Animations were created to show a 360 degree rotation of the composite, and thus give insight into the damage distribution and form in three dimensions. Table 3 expresses the number of active voxels associated with matrix cracks as a percentage of the number of active voxels in the solid body, thus quantifying the difference in the amount of damage detected when the specimen was held at P_{max}, and after unloading at P_0. The final representations of cracking and closure in Figure 7 include views from the face and edge orientations.

Table 3. Voxel measurements of damage (cracks) detected at P_{max} and P_0, N = 650.

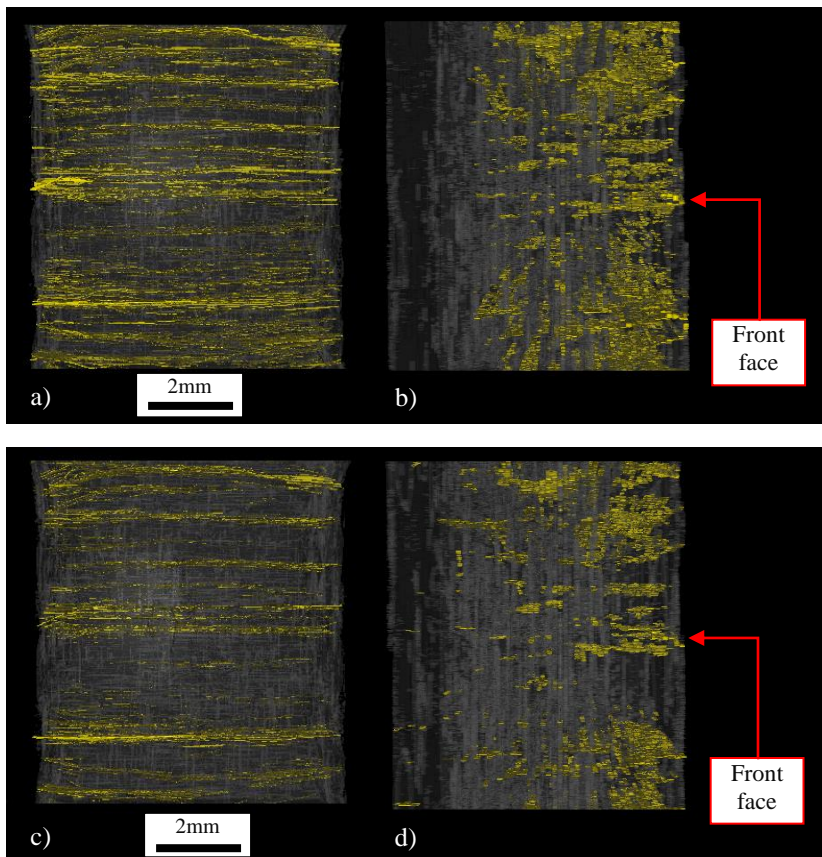|	N = 650, P_{max}	N = 650, P_0
Active voxels in Object 1 (i.e. cracks)	230,245	114,284
Active voxels in Object 2 (i.e. solid surrounds)	22,134,014	22,667,808
Crack volume as % of solid body	**1.04%**	**0.50%**

Figure 7. Three-dimensional visualisation of subsurface crack networks; a) cycle 650 P_{max}, orientation normal to front surface, b) cycle 650 P_{max}, edge view rotated 90° around y-axis, c) cycle 650 P_0, orientation normal to front surface, d) cycle 650 P_0, rotated 90° around y-axis.

4. Discussion

Attempts to quantify the subsurface damage introduced into a SiC_f/SiC CMC after a selected number of tensile fatigue load cycles using in situ XCT have been presented. The detected damage was in the form of a complex network of matrix cracks, orientated near orthogonal to the tensile load axis. Damage was quantified by counting the number of voxels associated with open space and performing correlations at different load conditions. This combination of in situ XCT and volumetric analysis produces superior visualisations of internal cracks in a 3-dimensional space, and provides an overview of the true variation in crack distribution through the thickness of the specimen. For the purposes of this paper quantification results are quoted as percentages, but in all cases the voxel dimensions are known and measurements can be converted to units of volume if appropriate.

The first quantification technique represented by Figures 4 to 6 was comparatively time-efficient, however the damage visualisation capability is severely limited. The reference scan of the specimen, containing no mechanically induced damage, was compared against the scan after 650 load cycles, whilst the specimen was held at P_{max}. In the latter case, the contribution of open space due to new cracks was quantified as 0.64% of the total number of voxels in the 3-D space.

These measurements are naturally subject to experimental errors. For instance, the correlation between any two individual images would be sensitive to spatial errors in either of the x, y or z axes or variations in the image quality between scans. Any alteration in the XCT system settings, reconstruction software settings and image stack preparation can also result in minor variations in the grayscale distribution, and should be carefully controlled to ensure that the subsequent application of a threshold in SPIERS Edit is consistent.

The manual image manipulation required to construct Figure 7 was more time-consuming, but provided visually superior results. This method was employed to highlight the effects of crack closure during a single load cycle. The technique itself has the benefit of quantifying damage from a single scan – no reference data was required. Moreover, the volume occupied by cracks is expressed as a percentage of the volume of solid material, excluding the surrounding space. At P_0 the volume of the specimen occupied by visible, open cracks was calculated as 0.50%, whereas at P_{max} this approximately doubled to 1.04%. There were two contributing factors to this increase: firstly, some fractures exhibited a greater crack opening displacement under loading at P_{max}, and secondly some cracks closed to the extent that they were no longer visible at the resolution of the XCT scan after the removal of load. With the potential application of XCT inspection for condition monitoring during service in mind, this was a crucial finding from the present study. Service inspections would invariably be applied to components in the unloaded state. Hence, the detection of non-load bearing cracking could be subject to a volumetric error of the order of 50%.

The accumulation of permanent strain damage in CMCs under fatigue cycles has been previously reported, either through strain ratchetting measured at the peak of the stress-strain hysteresis loops [15] or at the trough of the cycle [3]. The former mechanism could be indicative of irreversible fibre/matrix sliding, whilst the latter could be caused by debris wedging the cracks open [16]. Either mechanism supports the XCT capability in detecting the permanently open cracks even under zero load.

Progressive opening of cracks under cyclic fatigue is linked to decreasing interfacial shear stresses at the fibre/matrix interface, caused by progressive wear along the de-bonded interface where fibres bridge a transverse matrix crack. While the resolution of the in situ XCT technique here was insufficient to identify interfacial cracks and de-bond lengths, the quantified measure of crack opening space may aid the validation of analytical shear-lag models [17,18]. Such 2-D crack opening measurements have previously been achieved through surface SEM imaging [13], and XCT imaging of mini-composite specimens [19]. Since the damage volume measured here is a function of crack length, width and opening displacement, further manual segmentation would be required in order to extract relevant data. However, if matrix cracking has saturated, any further increase in damage volume must be directly proportional to crack opening and thus a reduction in global interfacial shear stress. Some degree of error associated with the voxel size would be expected.

The now well established use of XCT imaging applied to interrupted or in situ fatigue tests has proven that a significant amount of matrix cracking is experienced during the very first loading half cycle (subject to the magnitude of the maximum applied stress). This can be confirmed through the employment of acoustic emission monitoring. Identical test conditions to those applied to the in situ fatigue tests reported above were employed on a CMC coupon of the same CMC variant but loaded in a standard laboratory test rig. As previously published [7], AE sensors were interfaced to the specimen and the onset of damage accumulation monitored as a function of cycles, Figure 8. A distinct and immediate increase in accumulated AE energy was recorded during the first load cycle. Subsequent cycles then displayed a much lower rate of damage accumulation through to the termination of the test at 650 cycles. These results have prompted modifications to the Deben facility to obtain contemporary characterisation of mechanical damage via AE and CT monitoring during in situ XCT testing.

It is unclear whether matrix crack saturation had been achieved during the present experiment. The energy trend from the supporting AE test in Figure 8 suggests that minimal cracking activity persisted towards cycle 650, yet the cracks visible in the XCT images do not appear to extend through the entire thickness of the specimen. Sudden step-increases in AE energy have been observed in specimens subjected to relatively higher cycle numbers [7], so further crack propagation could be expected beyond the number of cycles investigated here.
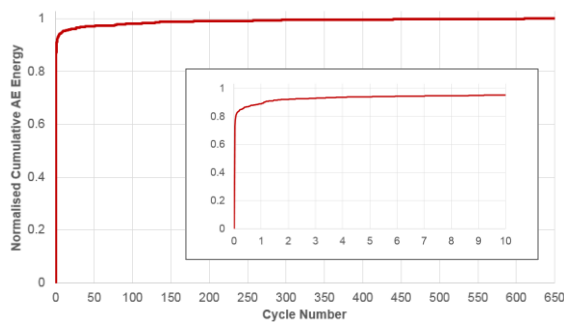

Figure 8. Cumulative AE energy curve from a standard SiC$_f$/SiC CMC specimen (Inset: initial 10 cycles).

The 3-D visualisation results presented in Figure 7 clearly highlighted a significant bias in crack density towards the 'front' surface of the specimen. The surface roughness of the opposing faces of the processed panel had been deliberately varied, with the woven fibre architecture more prominent on the front surface. The relatively reduced layer of silicon carbide to the front surface as shown in Figure 2 when compared to the rear face produced more prominent recesses between the woven fibre bundles. These localised stress raising features appear to be responsible for the preferential initiation of the matrix cracks. Careful attention was given to the alignment of the specimens in the Deben load train and samples were deliberately clamped with the front and rear faces reversed in the grips during successive tests to counter any effects of bending stresses. Further research into surface condition and the effects on damage initiation, particularly in association with environmental coatings, deserves consideration.

In general, the imaging techniques explored here offer potential for improved visualisation and assessment of matrix cracking within CMC specimens. The future direction of our research is now expected to advance our use of 2-D digital image correlation based on in situ surface observations [7] into full 3-D digital volume correlation

(DVC) employing XCT imaging [20], in order to develop a greater understanding of constitutive damage in CMCs.

5. Conclusions

- Damage in the form of matrix cracking has been visualised in three dimensions on a macroscopic scale using in situ XCT inspection of fatigue test coupons.
- Quantitative measurements of the volume of damage can be achieved through the employment of greyscale threshold techniques applied to the 3-D XCT scans.
- The same imaging techniques can characterise crack closure during a single fatigue cycle.
- The crack closure phenomenon poses important implications for the potential use of XCT inspection to detect damage in engineering components.
- A combination of XCT and AE monitoring has confirmed that significant matrix cracking may be introduced during the first load cycle of a fatigue test.

Acknowledgements

References

[1] A. Kelly, Concise Encyclopedia of Composite Materials, Elsevier, Dec 2012.

[2] M. R. Bache, J. P. Jones, Z. Quiney and L. Gale, "Damage Development in SiCf/SiC Composites Through Mechanical Loading," in *Proceedings of ASME Turbo Expo 2017*, Charlotte, NC, USA, 2017.

[3] E. Weston, P. I. Nicholson, S. Pattison and M. R. Bache, "Mechanical Damage Accumulation in SiCf/SiC CMCs Characterised via In Situ Computed X-ray Tomography," in *Proceedings of ASME Turbo Expo 2019*, Phoenix, Arizona, USA, 2019.

[4] M. R. Bache, P. I. Nicholson and E. Williams, "In-Situ Assessment of Fracture in SiCf/SiC under Computed X-ray Tomography," in *Proceedings of ASMA Turbo Expo 2018*, Oslo, Norway, 2018.

[5] C. Chateau, L. Gelebart, M. Bornert, J. Crepin, E. Boller, C. Sauder and W. Ludwig, "In Situ X-ray Microtomography Characterization of Damage in SiCf/SiC Minicomposites," *Composites Science and Technology,* vol. 71, pp. 916-924, 2011.

[6] E. Maillet, A. Singhal, A. Hilmas, Y. Gao, Y. Zhou, G. Henson and G. Wilson, "Combining in-situ synchrotron X-ray microtomography and acoustic emission to characterize damage evolution in ceramic matrix composites," *Journal of the European Ceramic Society,* vol. 39, pp. 3546-3556, 2019.

[7] M. R. Bache, C. D. Newton, J. P. Jones, S. Pattison, L. Gale, P. I. Nicholson and E. Weston, "Advances in Damage Monitoring Techniques for the Detection of Failure in SiCf/SiC Ceramic Matrix Composites," *Ceramics,* vol. 2, pp. 347-371, 2019.

[8] S. Momon, N. Godin, P. Reynaud, M. R'Mili and G. Fantozzi, "Unsupervised and supervised classification of AE data collected during fatigue test on CMC at high temperature," *Composites: Part A,* vol. 43, pp. 254-260, 2012.

[9] E. Maillet, M. P. Appleby and G. N. Morscher, "Health monitoring of Ceramic Matrix Composites from waveform-based analysis of Acoustic Emission," *MATEC Web of Conferences: Testing and Modeling Ceramic & Carbon Matrix Composites,* vol. 29, 2015.

[10] G. N. Morscher and N. A. Gordon, "Acoustic emission and electrical resistance in SiC-based laminate ceramic composites tested under tensile loading," *Journal of the European Ceramic Society,* vol. 37, pp. 3861-3872, 2017.

[11] N. Godin, P. Reynaud and G. Fantozzi, "Contribution of AE analysis in order to evaluate time to failure of ceramic matrix composites," *Engineering Fracture Mechanics,* vol. 210, pp. 452-469, 2019.

[12] Z. Quiney, M. R. Bache and J. P. Jones, "Inspection of SiCf/SiC Ceramic Matrix Composite Specimens Employed for Fatigue Experiments via Laboratory X-Ray Computed Microtomography," in *7th International Symposium on NDT in Aerospace*, Bremen, 2015.

[13] S. P. Jordan, M. R. Bache, C. D. Newton and L. Gale, "Characterisation of SiCf/SiC specimens using an in-situ tensile stage within a scanning electron microscope," in *Proceedings of ASME Turbo Expo*, 2019, 2019.

[14] G. N. Morscher, M. Singh, J. D. Kiser, M. Freedman and R. Bhatt, "Modeling stress-dependent matrix cracking and stress–strain behavior in 2D woven SiC fiber reinforced CVI SiC composites," *Composites Science and Technology,* vol. 67, no. 6, pp. 1009-1017, 2007.

[15] P. Reynaud, "Cyclic Fatigue of Ceramic-Matrix Composites at Ambient and Elevated Temperatures," *Composites Science and Technology,* vol. 56, pp. 809-814, 1996.

[16] R. O. Ritchie, "Mechanisms of fatigue-crack propagation in ductile and brittle solids," *International Journal of Fracture,* vol. 100, pp. 55-83, 1999.

[17] L. Longbiao, "Fatigue Life Prediction of Fiber-Reinforced Ceramic-Matrix Composites with Different Fiber Preforms at Room and Elevated Temperatures," *Materials,* vol. 9, no. 3, p. 207, 2016.

[18] L. Longbiao, "Synergistic effects of fiber debonding and fracture on matrix cracking in fiber-reinforced ceramic-matrix composites," *Materials Science and Engineering: A,* vol. 682, pp. 482-490, 2017.

[19] C. Chateau, L. Gelebart, M. Bornert, J. Crepin, D. Caldemaison and C. Sauder, "Modeling of damage in unidirectional ceramic matrix composites and multi-scale experimental validation on third generation SiC/SiC minicomposites," *Journal of the Mechanics and Physics of Solids,* vol. 63, pp. 298-319, 2014.

[20] L. Saucedo-Mora, T. Lowe, S. Zhao, P. D. Lee, P. M. Mummery and T. J. Marrow, "In situ observation of mechanical damage within a SiC-SiC ceramic matrix composite," *Journal of Nuclear Materials,* vol. 481, pp. 13-23, 2016.